The emergence of dissipation dilution

in doubly clamped nanomechanical resonators

by

J.C. van der Zalm

to obtain the degree of Bachelor of Science
at the Delft University of Technology,
to be defended publicly on Monday July 22, 2019 at 10:00 AM

Student number:	4440943	
Project duration:	April 23, 2018 – July 6, 2018	
	April 1, 2019 – July 22, 2019	
Thesis committee:	Prof. dr. G.A. Steele,	TU Delft, supervisor
	Prof. dr. P.G. Steeneken,	TU Delft, second examiner

This thesis is confidential and cannot be made public until July 22, 2019.

TU Delft

Preface

I would not have been able to have written this thesis if the foundation of beam theory wasn't developed first. Often the analytical attempt to determine the load carrying capacity of a transversely loaded beam by Galileo is seen as the beginning of beam theory. After which great minds like Mariotte, Bernoulli, Euler, Parent and Saint-Verant and others continued the progress [1]. Though hard to find in any textbook, Leonardo da Vinci made a fundamental contribution to what is commonly referred to as Euler-Bernoulli beam theory 145 years before Galileo.

Leonardo wasn't that well versed in mathematics, but by making the right basic assumption he was able to hypothesize the form of strain distribution two centuries before Bernoulli. Da Vinci established all of the essential features of the strain distribution in a beam by pondering the deformation of springs. He considered the case of a rectangular cross-section, he argued that there should be equal tensile and compressive strains at the outer fibres, and that there should be a neutral surface in the middle as well as a linear strain distribution.

Hooke's law as well as calculus were not yet discovered back then. If Leonardo would have had those tools, it is conceivable that he would have been able to lay the foundations for the now known Euler-Bernoulli beam theory.

Unlike Leonardo, Galileo made the wrong assumption that the stress across the cross-section of the beam is uniform. Which goes to show that Leonardo's straightforward hypothesis is even more remarkable. He was known to write in books that he carried with him at all times on a daily basis, and from these notes manuscripts have been formed. His notes on the bending of springs can be seen in the figure on the next page.

This thesis is written as part of the Applied Physics bachelor programme given at the faculty of Applied Sciences at the Delft University of Technology. I have benefited from the comments and advice of my supervisor G.A. Steele, who pointed out weaknesses (or errors) while I was writing my thesis. During our discussions he would clearly explain the physics and supplied interesting phenomena.

J.C. van der Zalm
Delft, July 2019

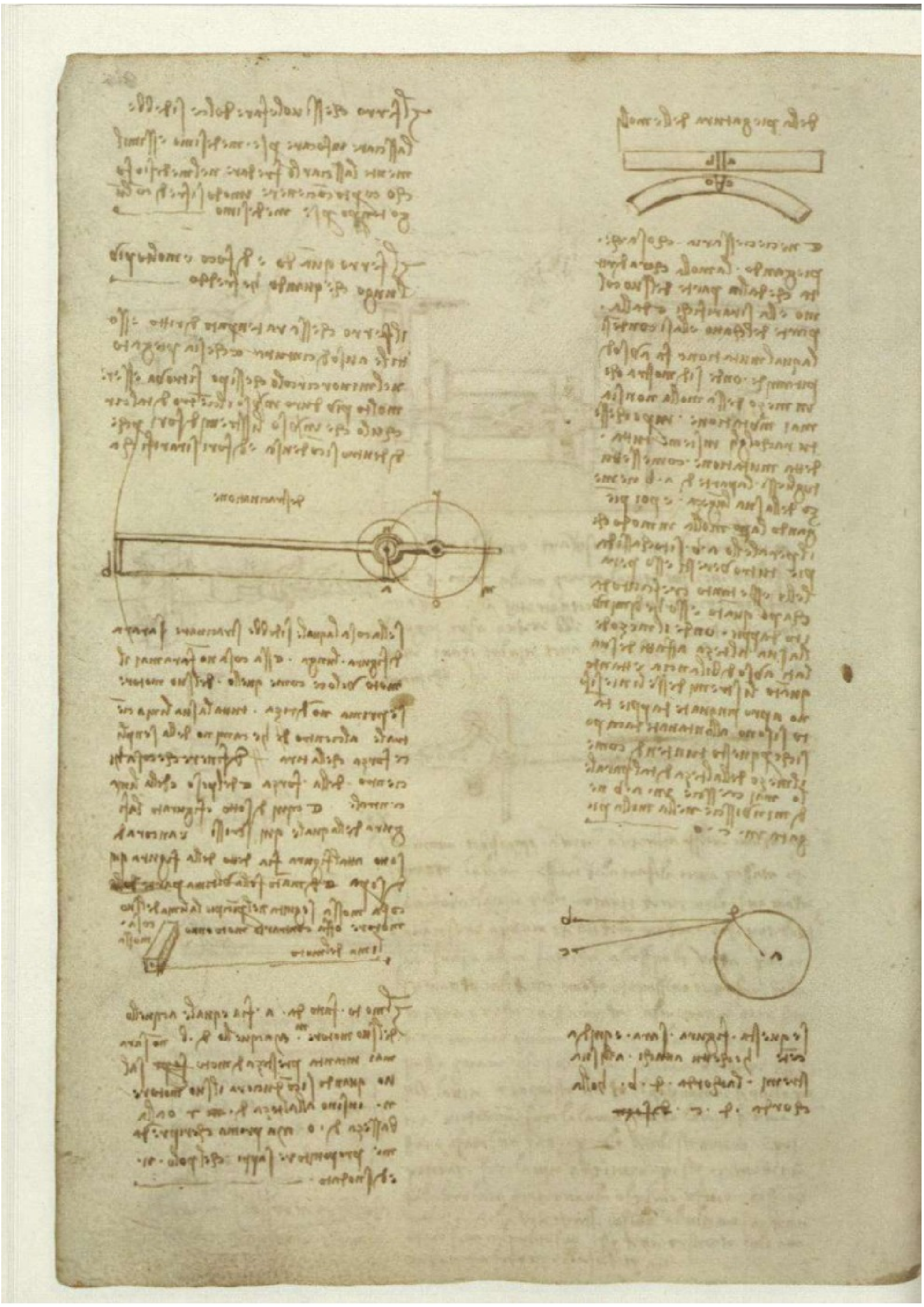

Figure 1: The notes of Leonardo da Vinci on the bending of springs in the top right corner, a digital scan taken from the 84th page of the Codex Madrid I [2].

Contents

1
Introduction

Doubly clamped nanomechanical resonators are quite comparable to the strings on a guitar. But unlike the tiny resonators, the guitar strings are tangible. You can even make the waves in these strings visible by illuminating them with light of the right frequency. An example of such a picture can be seen in figure 1.1.

But as you can see in the figure, the distance between the crests and troughs varies, some waves are longer than others. And as they travel along the guitar, at a specific spot on the string, that part will move up and down, depending on what part of the wave is passing by. The time it takes between two passing crests determines how fast the string is vibrating, the frequency of the wave.

It is this frequency that we can hear, the pitch of the guitar string. The faster the string is oscillating the higher the pitch will be that you hear. For the musician using the guitar it is rather important that the song he plays is harmonious. So he would like to be able to tune his guitar. To do this he can tighten and loosen the strings. By rotating the machine heads on the headstock he can increase and decrease the tension in the strings. In this way the pitch of the sound they produce can be altered.

How does this relate to the little nanomechanical resonator? It turns out that in the same way as the guitar, the nanomechancial resonator can also be tuned. But this does not only change the frequency at which it vibrates, it also changes the resonance behaviour and the qualitative damping process. And similar to the harmony that the musician was seeking, a physicist would like to optimize his resonator. But what does the physicist use his resonator for? Well, it's not so that he can play *Sultans Of Swing*, that is for sure.

1.1. Application example

The most likely example can be found in sensing. There are plenty of examples of sensors that use vibrating components, because there are plenty of reasons where you would want to know how something is vibrating, or how the vibration changes over time. But to make it more clear here is an example.

Let's say that you want to precisely track the mass of an object while you are also in orbit around Earth. There is no way you can use a traditional balance as the weight of the object depends on the gravitational pull. And dealing with the change of gravity while you are in orbit would be quite difficult. But, by making the object oscillate using an *inertial balance* the mass can be determined as the frequency of the vibration will depend on the unknown mass.

So, if the mass changes, the frequency of the vibration will also change. However, often it isn't one frequency that is measured, but a distribution of frequencies. With a peak around the resonance frequency of the vibrating mass-spring system. By changing the resonance behaviour and the qualitative damping process it is possible to get a narrower band of frequencies. And because the peaks are narrower, it is easier to distinguish between them. This essentially enables the physicist to make a more precise measurement of the change in frequency. Which ultimately makes it possible to calculate the change in the object's mass over time more accurately.

1.2. Outline

In this thesis the transition between high and low amounts of damping in doubly clamped nanomechanical resonators is investigated. In the next chapter a brief look is taken to the existing literature. Thereafter the different types of damping are investigated in chapter 3. Then in chapter 4 a model for a damped nanomechancial beam, as well as the procedure to derive it, will be discussed. The conclusions of this investigation can be found in the final chapter, chapter 5.

Figure 1.1: Waves in guitar strings, it is even possible to observe the overtones in the first E string, the thickest string on the bottom. The wave is build up out of multiple different frequencies occuring on the same string [3].

2

Background

The resonant motion of nanoelectromechanical systems has already received a lot of attention over the years. This results in a vast amount of articles on this topic, containing experimental results and theoretical findings. From that collection of scientific work two articles will be discussed. Starting of with the oldest of the two: *Damping of Nanomechanical Resonators* [4].

2.1. The experimental facts

In their paper they describe how they were able to predict the observed mode-dependent damping with a single frequency-independent fit parameter. At that time there was no satisfactory understanding of the origin of structural damping. But their model is able to clarify the role of tensile stress on damping, it also gives a hint of the underlying microscopic mechanisms.

They were able to do this by assuming that the local strain induced by the resonator's displacement causes the damping. So that the high quality factors of strained nanosystems is due to the increase in stored elastic energy rather than a decrease in energy loss. In their experiments they have studied nanomechanical beams fabricated from high stress silicon nitride. They vary the resonance frequency of the beams by changing the length. To reproduce the measured frequency spectrum they apply the standard beam theory. Then they calculate the strain distribution within the resonator and the accompanying energy loss. They find that the energy loss is determined by two sources. The elongation of the beam and its local bending. But the former has a negligible contribution. After that the quality factor is calculated, which depends on the amount of stored energy.

They can reproduce all measured quality factors by assuming that the Young's modulus imaginary part is independent of the resonators length and harmonic mode. If two beams of equal resonance frequency are compared, one of which is shorter but oscillating at a higher mode, they find that the longer beam oscillating at a lower mode has a higher quality factor. This is attributed to the *experimental fact* that the maximum strain occurs near the clamping points and a beam oscillating at a higher mode has less clamping points per anti-node.

In a relaxed beam the elastic energy is stored in the flexural deformation which is proportional to the energy loss in Zener's model. Because of this proportionality the quality factor is frequency independent for the unstressed beam. In stressed beams however there is a stronger dependence of the quality factor on the resonance frequency. They find that the stored elastic energy in the beam can be seperated into two parts. One linked to the bending and the other to the overall elongation. The elongative stored energy is found to be proportional to the prestress and vanishes for relaxed beams. They conclude by the finding that the mechanism comes from the interaction of the strain with local defects of which they hadn't identified the origin yet.

2.2. Applying strain engineering

In more recent work, *Elastic strain engineering for ultralow mechanical dissipation* [5], it is shown how nanoscale stress can be used to realize exceptionally low mechanical dissipation when combined with soft-clamping. By doing this they were able to obtain super high quality factors, as high as 800 million.

The engineering of elastic strain to obtain resonators with low dissipation is also known as dissipation dilution. The stiffness of a stressed material is increased without added losses. By reducing the system dimension a smaller mass resonator can be created which can improve the dissipation dilution to obtain higher quality factors.

The other approach to obtain higher Q values is to rely on the extreme inhomogeneous stresses produced by nanoscale deformation. It is difficult to design such a system that you utilize both of these approaches. In their paper they describe what their strategy was to bring these approaches together. They created a band gap for localizing the flexural modes around a central defect. By tapering the beam, they colocalize the modes with a region of enhanced stress.

They illustrate the main features of their approach by first looking at a model where they vary the width of a beam along its length. They determine the amount of energy that is stored in the bending and elongation of the beam. After that they determine the enhancement to the Q due to an increase in the stress. They call this the "dilution factor". But most stressed nanomechanical resonators that have been studied operate below this limit. This is due to the clamping loss. Due to the boundary conditions there is extra curvature at the clamping sites. This together with the antinodes reduces the dilution factor.

The Q factor could be increased in several ways. The fundamental modes typically have a higher Q. Another way would be to increase the aspect ratio of the beam, making it longer and less high. You could also increase the stress in the beam. There is also another more complex way, by using periodic micropatterning to localize the mode shape away from the supports. This is also called a phononic crystal, which can greatly suppress certain modes.

They apply both soft clamping and the colocalization of the mode shape with a region of geometrically enhanced stress. They warn for the fact that the stress is only enhanced in a small area, so that means that high-order flexural modes must be used to achieve sufficient colocalization. They achieve this by tapering the width of unit cells on the string toward the defect in the middle. This tapering is done according to a Gaussian envelope function.

First they study the untapered nanoresonators of different lengths. They find that the mode frequencies agree well with the 1D Euler-Bernoulli equation. They also find that there are very few modes within the band gap. Inside this band gap the Q approaches that of an idealized clamp-free beam. After establishing this near-ideal soft-clamping of uniform nanobeams they study the performance of tapered nanobeams. They do this by varying the length of the taper, this will tune the stress at the center of the beam. By doing this they find higher Q values, about three times as high then without the tapering. Using even longer beams they found their highest recorded Q values.

They reflect that they were not operating at the limiting yield stress, so they could have fabricated beams with even higher stresses. By using this as well as even higher aspect ratios the Q factor could be increased even further. Similarly to the other discussed article here they conclude that the source of intrinsic loss in their devices is unknown but it is likely due to surface imperfections.

3

Damping models for a simple mass-spring system

In this chapter four different damping models for a simple mass-spring system will be studied. Starting of with the well-known viscous damped system.

3.1. Viscous damping

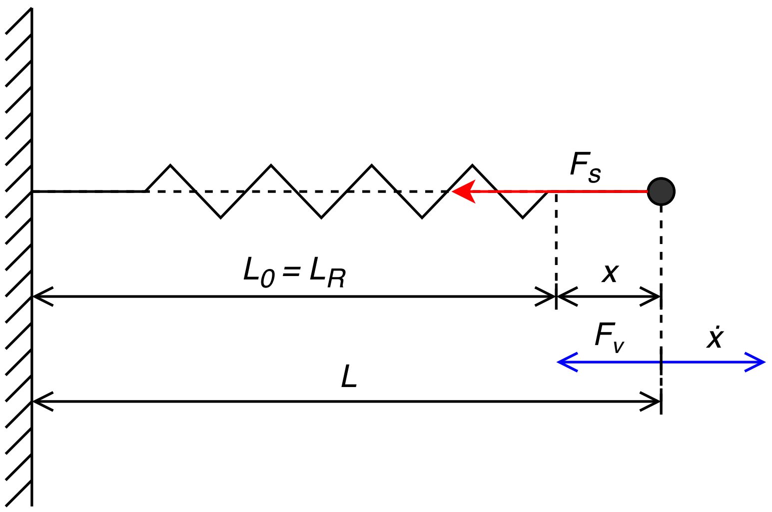

Figure 3.1: Schematic overview of the viscous damped mass-spring system.

In figure 3.1 a schematic drawing of the oscillating mass attached to a wall with a spring can be seen. The mass can only move in the x-direction. The starting position is L_0 which is equal to the rest length L_R. The difference between the rest length and the position of the mass is defined to be x. It is assumed that the spring rate k is linear, so that the spring force is calculated as follows.

$$F_s = -k(L - L_R) = -kx \tag{3.1}$$

Besides the spring force there is also a viscous velocity proportional damping force F_v, given by the following equation.

$$F_v = -c\dot{x} \tag{3.2}$$

With c being the viscous damping coefficient. To determine the equations of motion of the mass Newton's second law of motion can be applied.

$$m\ddot{x} = \sum_i F_i = -kx - c\dot{x} \tag{3.3}$$

Obtaining the following second order linear homogeneous differential equation with constant coefficients.

$$m\frac{d^2}{dt^2}x + c\frac{d}{dt}x + kx = 0 \tag{3.4}$$

3.1.1. Finding the solution

Solving equation 3.4, and finding a formula for x, is quite straightforward, starting with the following ansatz.

$$q(t) = \alpha\, e^{\lambda t+\varphi};\quad \dot{q}(t) = \alpha\lambda\, e^{\lambda t+\varphi};\quad \ddot{q}(t) = \alpha\lambda^2\, e^{\lambda t+\varphi} \tag{3.5}$$

As is usual, this educated guess that is postulated here will later be verified by its results. Plugging in the ansatz for x into equation 3.4 the following is derived.

$$\begin{aligned} m\alpha\lambda^2\, e^{\lambda t+\varphi} + c\alpha\lambda\, e^{\lambda t+\varphi} + k\alpha\, e^{\lambda t+\varphi} &= 0 \\ \left(m\lambda^2 + c\lambda + k\right)\alpha\, e^{\lambda t+\varphi} &= 0 \\ m\lambda^2 + c\lambda + k = 0 \quad \vee \quad \alpha = 0 \;\; &\text{(The trivial solution)} \end{aligned} \tag{3.6}$$

Besides the trivial solution, using the quadratic formula, two solutions for λ can be found.

$$\lambda_\pm = -\frac{c}{2m} \pm \frac{1}{2m}\sqrt{c^2 - 4mk} = -\frac{c}{2m} \pm i\sqrt{\frac{k}{m} - \frac{c^2}{4m^2}} \tag{3.7}$$

If the value 0 is filled in for c the angular frequency ω_0 for an undamped mass spring system can be found.

$$\lambda_\pm = \pm i\sqrt{\frac{k}{m}} = \pm i\omega_0 \Rightarrow \omega_0 = \sqrt{\frac{k}{m}} \tag{3.8}$$

Equation 3.7 can be simplified by using the damping ratio defined as: $\zeta = \frac{c}{2\sqrt{km}}$, and it can further be simplified symbolically.

$$\lambda_\pm = -\omega_0\left(\zeta \mp i\sqrt{1-\zeta^2}\right) \tag{3.9}$$

Now only λ_+ is considered because for λ_- the amplitude would increase exponentially towards infinity. What is found here is complex valued. By inserting this back in the ansatz and taking the real part a general solution for x is found.

$$x(t) = \Re\mathfrak{e}\left\{\alpha\, e^{-\omega_0\zeta t+\varphi}\, e^{i\omega_0\sqrt{1-\zeta^2}\,t}\right\} \tag{3.10}$$

Depending on the value of ζ three different cases can be distinguished:

1. *Overdamped* ($\zeta > 1$)
2. *Critically damped* ($\zeta = 1$)
3. *Underdamped* ($0 \leq \zeta < 1$)

3.1.2. Loss tangent & Quality factor

The loss tangent $\tan(\delta)$ can be calculated with the following equation.

$$\tan(\delta) = \frac{c\omega}{m\omega_0^2} \rightarrow \tan(\delta) = 2\zeta \text{ if } (\omega = \omega_0) \tag{3.11}$$

This equation is obtained by looking at the definition of the loss tangent for an oscillation with structural damping, and rewriting the terms responsible for the damping to viscous terms. Right now this comes out of thin air, it will become more evident in the next section, section 3.2, where structural damping of this spring system is discussed. The quality factor Q can be easily calculated from $\tan(\delta)$ in the following way.

$$Q = \frac{1}{\tan(\delta)} = \frac{m\omega_0^2}{c\omega} \rightarrow Q = \frac{1}{2\zeta} \text{ if } (\omega = \omega_0) \tag{3.12}$$

3.2. Structural damping

In this section structural damping is introduced. This is done by extending Hooke's law to include an imaginary spring constant term responsible for internal damping [6].

$$F_s^{in} = -k\left[1 + i\phi(\omega)\right]x \tag{3.13}$$

Newton's laws of motion can again be applied to obtain the equations of motion, but in this case F_s^{in} includes both the spring force and friction force. With the angle $\phi(\omega)$ being responsible for the structural damping, it should be taken in such a way that the energy dissipated in each oscillation period is the same, independent of the frequency. Because $\phi(\omega)$ is a function of ω it now makes sense to apply a Fourier transformed version of Newton's second law of motion.

$$\mathscr{F}\{m\ddot{x}\} = \mathscr{F}\left\{\sum_i F_i\right\} = \mathscr{F}\left\{F_s^{in}\right\} = -k\left[1 + i\phi(\omega)\right]X(\omega) \tag{3.14}$$

Writing this out the following algebraic equation for $X(\omega)$ can be found.

$$m(i\omega)^2 X(\omega) + k\left[1 + i\phi(\omega)\right]X(\omega) = 0 \tag{3.15}$$

3.2.1. Finding the solution

The next step will be to solve equation 3.15 and obtain a formula for $x(t)$. The previous ansatz from equation 3.5 can be used, as well as its Fourier transform.

$$q(t) = \alpha\,\mathrm{e}^{\lambda t + \varphi}; \quad \mathscr{F}\{q(t)\} = \frac{1}{2\pi}\int_{-\infty}^{\infty} \alpha\,\mathrm{e}^{\lambda t + \varphi}\,\mathrm{e}^{i\omega t}\,dt = \alpha\delta(\omega - i\lambda)\,\mathrm{e}^{\varphi} \tag{3.16}$$

The following calculations are quite similar as those done before for viscous damping. Equation 3.15 can be simplified by factoring out the $X(\omega)$ term.

$$\begin{aligned} m(i\omega)^2 X(\omega) + k\left[1 + i\phi(\omega)\right]X(\omega) &= 0 \\ \left(m(i\omega)^2 + k\left[1 + i\phi(\omega)\right]\right)X(\omega) &= 0 \\ m(i\omega)^2 + k\left[1 + i\phi(\omega)\right] &= 0 \quad \vee \quad X(\omega) = 0 \text{ (The trivial solution)} \end{aligned} \tag{3.17}$$

From the trivial solution it can be seen that it holds only if $\omega \neq i\lambda$. In the case that $\omega = i\lambda$, a solution for λ can be obtained. Now it can also be checked if filling in the value 0 for $\phi(\omega)$ gives us the expected result, finding the undamped angular frequency ω_0.

$$\lambda_\pm = \pm i\sqrt{\frac{k}{m}}\sqrt{1 + i\phi(\omega)} = \pm i\omega_0\sqrt{1 + i\phi(\omega)} \Rightarrow \omega_0 = \sqrt{\frac{k}{m}} \tag{3.18}$$

It checks out! Now for the same reason as before only λ_+ is considered. Let's calculate the real and imaginary part of this eigenvalue so that these terms can be split. The square root is split using DeMoivre's

Theorem [7]. After that it can be further simplified by a Taylor expansion of $\sqrt{1+\phi^2(\omega)}$ for $\phi \ll 1$. This assumption is made so that the time average of the product $F\dot{x}$ is proportional to ϕ.

$$\begin{aligned}
\lambda_+ &= i\omega_0\sqrt{1+i\phi(\omega)} = i\omega_0\sqrt{z} = i\omega_0\sqrt{r(\cos(\theta)+i\sin(\theta))} \\
\text{with } r &= \sqrt{1+\phi^2(\omega)};\ \ \cos(\theta) = \frac{1}{r};\ \ \sin(\theta) = \frac{\phi(\omega)}{r} \\
\lambda_+ &= i\omega_0\left(\frac{\sqrt{2}}{2}\sqrt{\sqrt{1+\phi^2(\omega)}+1} + i\frac{\sqrt{2}}{2}\sqrt{\sqrt{1+\phi^2(\omega)}-1}\right) \\
\lambda_+ &\approx i\omega_0\left(\frac{\sqrt{2}}{2}\sqrt{1+\frac{\phi^2(\omega)}{2}+1} + i\frac{\sqrt{2}}{2}\sqrt{1+\frac{\phi^2(\omega)}{2}-1}\right) \\
\lambda_+ &\approx i\omega_0\left(\frac{1}{2}\sqrt{4+\phi^2(\omega)} + \frac{i}{2}\phi(\omega)\right) \approx i\omega_0\left(1+\frac{\phi^2(\omega)}{8} + \frac{i}{2}\phi(\omega)\right) \\
\lambda_+ &\approx -\frac{1}{2}\omega_0\phi(\omega) + i\omega_0\left(1+\frac{\phi^2(\omega)}{8}\right) \\
\mathfrak{Re}\{\lambda_+\} &\approx -\frac{1}{2}\omega_0\phi(\omega) \ \ \wedge \ \ \mathfrak{Im}\{\lambda_+\} \approx \omega_0\left(1+\frac{\phi^2(\omega)}{8}\right)
\end{aligned} \tag{3.19}$$

Thus for x the following is found:

$$x(t) \approx \alpha\, \mathrm{e}^{-\frac{1}{2}\omega_0\phi(\omega)\cdot t}\, \mathrm{e}^{i\omega_0\left(1+\frac{\phi^2(\omega)}{8}\right)\cdot t+\varphi} \tag{3.20}$$

Note that there is a new resonant frequency $\omega_{s,0}$ of the oscillation and it is given by: $\omega_{s,0} = \omega_0\left(1+\frac{\phi^2(\omega)}{8}\right)$. It depends on both ω_0 and $\phi(\omega)$.

3.2.2. Loss tangent & Quality factor

To determine the loss tangent and quality factor, of the springs described in this model, the spring constant has to be split in its purely real and imaginary parts.

$$k = k' - ik'' \tag{3.21}$$

Let's rewrite equation 3.17 to see what can be obtained for k' and k''

$$\begin{aligned}
0 &= m\lambda^2 + k\left[1+i\phi(\omega)\right] \\
k &= -\frac{m\lambda_+^2}{1+i\phi(\omega)} \\
k &= \frac{m\omega^2}{1+i\phi(\omega)}\left(\frac{1-i\phi(\omega)}{1-i\phi(\omega)}\right) \\
k &= \frac{m\omega^2}{1+i\phi(\omega)}\left(\frac{1}{1-i\phi(\omega)} - \frac{i\phi(\omega)}{1-i\phi(\omega)}\right) \\
k &= \frac{m\omega^2}{1+i\phi(\omega)}\frac{1}{1-i\phi(\omega)} - \frac{m\omega^2}{1+i\phi(\omega)}\frac{i\phi(\omega)}{1-i\phi(\omega)} \\
k &= \frac{m\omega^2}{1+\phi^2(\omega)} - i\frac{m\omega^2}{1+\phi^2(\omega)}\phi(\omega) \\
k &= \beta - i\beta\phi(\omega);\ \ \text{with } \beta \equiv \frac{m\omega^2}{1+\phi^2(\omega)} \\
k' &= \beta \ \ \wedge \ \ k'' = \beta\phi(\omega)
\end{aligned} \tag{3.22}$$

The lag function can now simply be found by dividing the k' into k''. What is found then is actually also what is defined as the loss tangent.

$$\phi(\omega) = \frac{k''}{k'} = \tan(\delta) \tag{3.23}$$

The Q-factor can now easily be calculated by inverting these variables as seen in equation 3.12. Looking back on how the loss angle $\phi(\omega)$ was introduced, it makes sense that the loss tangent is simply equal to $\phi(\omega)$.

Both the structural damping factor k'' and the viscous damping factor c, that has been introduced in the previous section are responsible for exponential decay of the wave modes in the spring system. But rather than losing energy to some extra-structural medium now the energy is lost due to the complex stiffness of the spring.

To compare the viscous damping and structural damping k' and k'' can be expressed in terms of m, ω and c. This is done by rewriting equation 3.6 and equation 3.17 to find the real and imaginary part of k.

$$\begin{aligned} m(i\omega)^2 + k_s\left[1+\phi(\omega)\right] &= m\lambda^2 + c\lambda + k_v \\ \text{with } k_s\left[1+\phi(\omega)\right] &= k' - ik'' \\ \text{and } k_v &= m\omega_0^2 \\ k' - ik'' &= m\omega_0^2 - ic\omega \\ k' = m\omega_0^2 \quad &\wedge \quad k'' = c\omega \end{aligned} \tag{3.24}$$

3.3. Standard anelastic solid

There is another way of representing the structural damping from section 3.2, using the standard anelastic solid. One way of doing this is shown in figure 3.2, it shows an arrangement of two springs and a dashpot. In this figure, k' stands for the relaxed spring constant, and the sum $k' + k''$ is called the unrelaxed spring constant. It was Zener who showed that from this model the following equation for ϕ can be found assuming that $\phi \ll 1$.

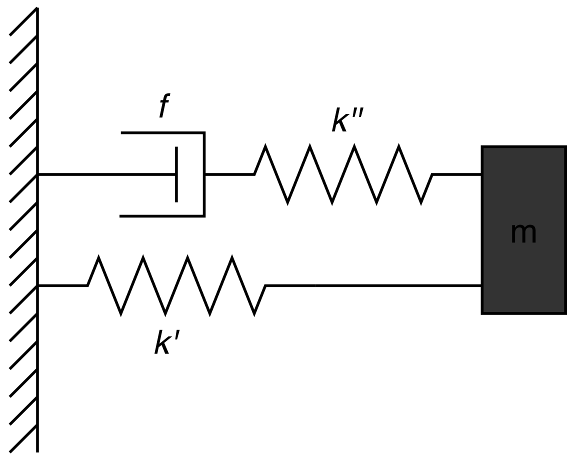

Figure 3.2: Schematic overview of a standard anelastic solid. An ideal spring is connected in parallel with a spring dashpot combination called a Maxwell unit, adapted from the article 'Thermal noise in mechanical experiments' [6, p. 2438].

$$\phi(\omega) = \Delta \frac{\omega\tau}{1+\omega^2\tau^2} \tag{3.25}$$

With $\Delta \equiv \frac{k''}{k'}$ the relaxation strength. Which is obtained from the Taylor approximation of $\tan(\delta)$ for small δ, and τ is called the relaxation time.

3.3.1. Loss tangent & Quality factor

The Q-factor can now easily be calculated by inverting the loss angle, again, similar to equation 3.12. Thus the following is found.

$$Q = \frac{1+\omega^2\tau^2}{\Delta\omega\tau} \tag{3.26}$$

3.4. Plots & Discussion

Loss tangent

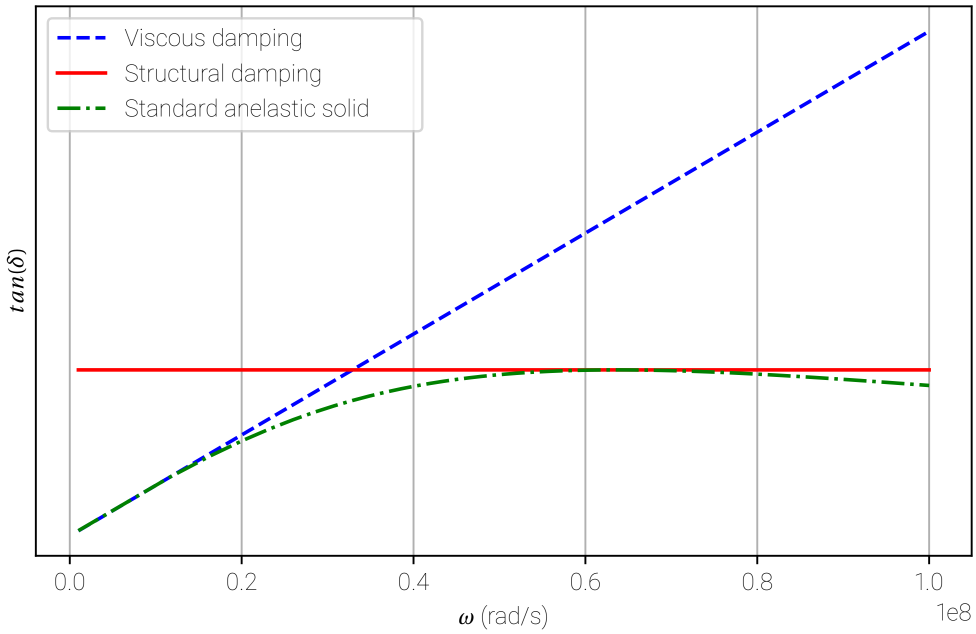

Figure 3.3: In this graph the loss tangents $\tan(\delta)$ of the discussed damping models are plotted versus the angular frequency ω. The loss tangents are dimensionless and the frequency is given in radians per second.

To visualize the calculations described in this chapter two figures have been made, using the values as described in table 3.1. Figure 3.3 shows the plots of $\tan(\delta)$ vs ω_0 for these models. By depicting the loss tangents of the models in this way the similarities and differences in their resonance behaviour can clearly be made visible.

Table 3.1: The parameters that were used to create both figure 3.3 and figure 3.4

Parameter	Variable	Value	Unit	Model
Length	l	100	µm	All
Width	w	2	µm	All
Height	h	2	µm	All
Density	ρ	2500	kg/m^3	All
Spring constant	k	1 to 10000	$N\,m^{-1}$	All
Damping coefficient	c	1×10^{-8}	$kg\,s^{-1}$	Viscous (3.1)
Loss angle	$\phi(\omega)$	1.57×10^{-4}	–	Structural (3.2)
Relaxation strength	Δ	3.14×10^{-4}	–	Standard anelastic solid (3.3)
Relaxation time	τ	1.57×10^{-8}	s	Standard anelastic solid (3.3)

The loss tangent of the viscous damping model, displayed as a blue dashed line, increases linearly with the frequency.

The loss tangent of the structural damping model is displayed as a red line. It is constant as the frequency increases. A frequency independent lag function is found in many kinds of material [6]. The physical origin behind this behaviour, were the lag function is approximately constant over a large band of frequencies, is still up to speculation. The constant lag function is consistent with the condition that it has to be an odd function of frequency provided that it doesn't stay constant to zero frequency.

The standard anelastic solid's tan (δ) is portrayed by the green dash-dotted line. For low frequencies it increases linearly, while for higher frequencies it decreases by one over the frequency towards zero. This type of lag-function does not show a discontinuity at zero frequency, and at a certain band of frequencies it's slope is similar to that of structural damping.

The quality factor

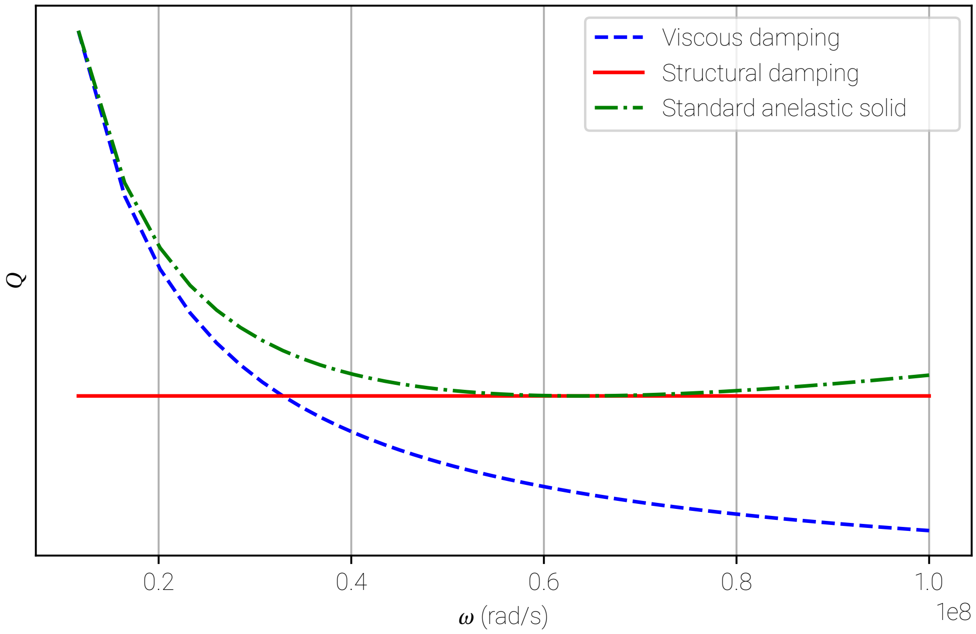

Figure 3.4: In this graph the Q-factors of the discussed damping models are plotted versus the angular frequency ω. The Q-factors are dimensionless and the frequency is given in radians per second.

Figure 3.4 shows the plots of Q vs ω for the described damping systems. This figure contains no new information compared to the other one but gives another perspective. In this way the qualitative damping process of the spring systems can be better compared.

The Q-factor of the viscous damping model, displayed as a blue dashed line, decreases with one over the frequency till zero. In high frequency systems where high Q is desirable the system has to be prepared in such a way that the viscous damping is decreased to the absolute minimum.

The Q-factor of the structural damping model is displayed as a red line. For this model the imaginary and real components of the spring constant differed only by the lag function. And because the lag function is constant for this model, the Q-factor is constant as well. At zero frequency, $\omega = 0$, the system does not oscillate and thus there is no Q-factor for this system to define there.

In the standard anelastic solid, something quite different can be observed. The Q-factor is displayed as the green dash-dotted line. It can be observed that the Q-factor of the standard anelastic solid follows the same trend as viscous damping at the lower frequencies. And after that for a certain band of frequencies it is quite similar to the constant Q-factor of structural damping. Then for higher frequencies the Q factor increases linearly towards infinity. By combining Maxwell units the band of frequencies, for which the solid behaves as if it is structurally damped, can be increased.

4

A mass on two springs: a model for a beam

The models that are discussed in this chapter can be used to study the forces and motion involved with the horizontal and vertical oscillation modes of doubly clamped beams. They are all formed by having a mass attached to two solid immovable walls with springs. In this chapter all springs are structurally damped, identical to the damping introduced in section 3.2. Let's first look at the simplest mass spring system, where the mass oscillates in the horizontal direction.

4.1. Stretching in horizontal motion

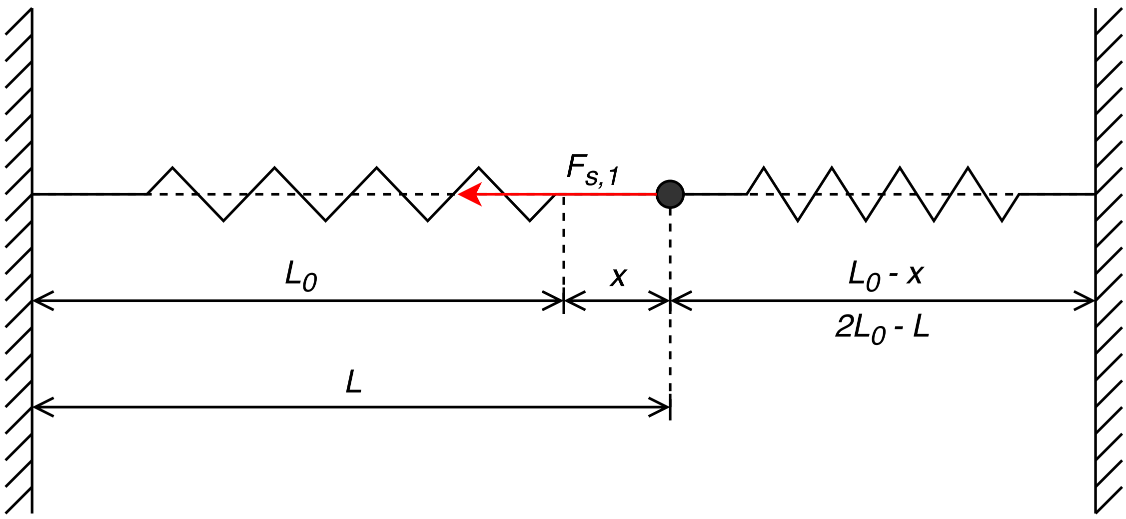

Figure 4.1: Schematic overview of the simple horizontal spring model. For ease of rendering $F_{s,2}$, the force due to the spring on the right, has not been drawn. The arrow for this force would look exactly the same as the one drawn for $F_{s,1}$.

4.1.1. Deformation

In figure 4.1 a schematic drawing can be seen of the oscillating mass attached with two springs. For this case, it is assumed that the mass only oscillates in the horizontal direction. It is also assumed that both springs have the same spring constant. Furthermore, it is assumed that both spring rates are linear. To justify that the model properly simulates beam oscillation this will be further analysed later on, in subsection 4.2.2. The distance from the centre to the mass is defined to be x. The expressions for the deformations of the springs are shown in figure 4.1 as well.

4.1.2. Restoring force

The restoring force, including both springs, is calculated as follows.

$$F_R = F_{s,1} + F_{s,2} = -k(L - L_R) + k(2L_0 - L - L_R) = -2k(L - L_0) = -2kx \tag{4.1}$$

It can be seen that the restoring force does not depend on the relaxed length L_R. This makes sense because the springs balance each other and only the residual force matters.

4.1.3. Structural damping

The solution to the equation of motion for a structurally damped spring has been found in the previous chapter in section 3.2. The only difference now is that there is not one but two springs pulling and pushing the mass. Both of the springs are structurally damped resulting in a new total restoring force.

$$F_R^{in} = -2k\left[1 + i\phi(\omega)\right]x \tag{4.2}$$

So the following differential equation is obtained.

$$m(i\omega)^2 X(\omega) + 2k\left[1 + i\phi(\omega)\right]X(\omega) = 0 \tag{4.3}$$

The only thing that changes from the previously obtained solution is the undamped angular frequency ω_0.

$$\omega_0 = \sqrt{\frac{2k}{m}} \tag{4.4}$$

Loss tangent & Quality factor

To obtain the loss tangent and the quality factor the same calculation as in section 3.2.2 can be repeated for this model. The result will be the same, a constant loss tangent and quality factor.

4.2. Stretching in transverse motion

4.2.1. Deformation

In figure 4.2 a schematic drawing can be seen of the oscillating mass attached with two springs. It is assumed that the mass is in the middle, located a distance L_0 from the sides. At a certain time t the mass is at height u, the springs connected to the mass now make an angle θ with the horizontal axis. By applying the Pythagorean theorem on the right triangles the length of the springs is given as follows

$$L^2 = L_0^2 + u^2 \tag{4.5}$$

This can be rewritten to obtain the following equation for the length.

$$L = L_0\sqrt{1 + \frac{u^2}{L_0^2}} \tag{4.6}$$

To further simplify equation 4.6 a Taylor expansion is done for the following situation: $L_0 \gg u$.

$$L \approx L_0\left(1 + \frac{u^2}{2L_0^2}\right) = L_0 + \frac{u^2}{2L_0} \tag{4.7}$$

It can now be observed that the spring length is the initial length plus an extra term. The extra term, the deformation of the spring with respect to L_0 is defined to be x.

$$x = L - L_0 \approx \frac{u^2}{2L_0} \tag{4.8}$$

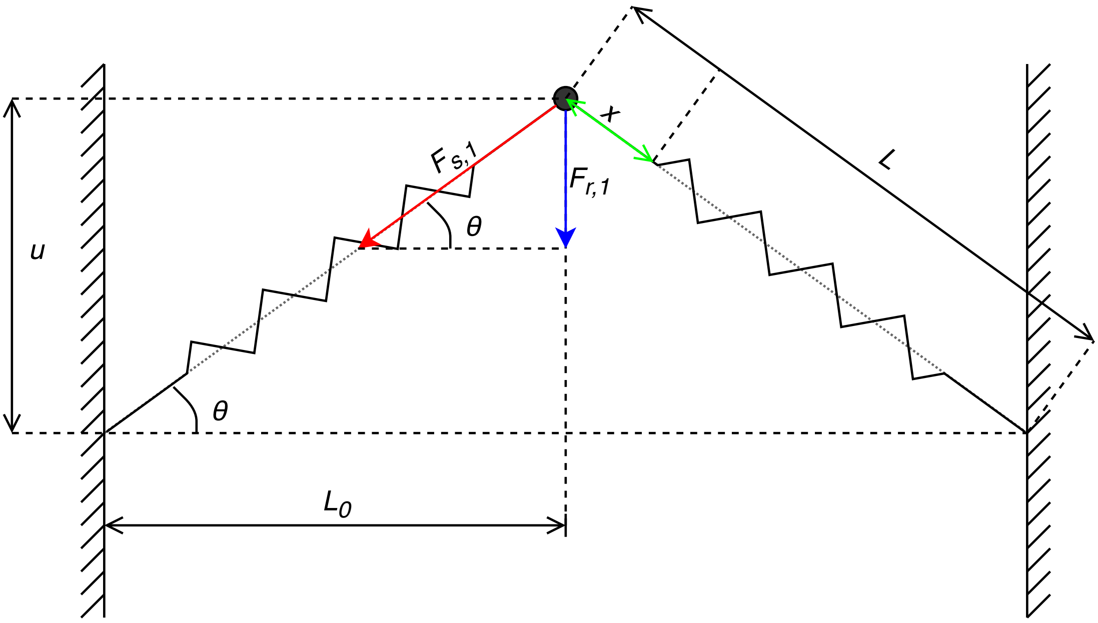

Figure 4.2: Schematic overview of the simple transverse stretching spring model. The forces due to the right spring have not been drawn for ease of rendering. $F_{s,2}$ would just be a mirrored version of $F_{s,1}$, mirroring about $x = L_0$. The vertical component $F_{r,2}$ would look exactly the same as $F_{r,1}$.

The approximation that was made here will be used throughout this model, it is important that this approximation can be justified for real experiments. Otherwise, the model described here would apply poorly to the real physical world that it tries to simulate. The justification can be found in the following section, section 4.2.2

4.2.2. Justification of the approximations

To justify the approximation $L_0 \gg u$ that is applied throughout this section an exemplary calculation will be done. The values that will be used in the calculation, while still being realistic, will be chosen to the detriment of the approximation. This is done to show that in the worst, yet realistic scenario, it still holds. For $\frac{u}{L_0}$ a value of 10^{-5} is found. This means that $L_0 \gg u$ is a good approximation up to that magnitude.

It is also assumed that the only relevant contributions of the restoring force are the linear ones. To justify this the stretching of the beam has to be very small. If this is the case, the linear response dominates the restoring force by a large margin. In other words, $x \approx 0$. Let's assume that the beam has a length of 50 microns, $L_0 = 50$µm and a pretty big vertical amplitude of 1 picometre, $u = 1$pm. From this the stretching along the beam can be approximated using formula 4.8. Doing this a value of $x \approx 10^{-17}$m is found.

A large nucleus is about 10 fm big (10^{-16}m). And since the stretching is one order of magnitude smaller than a big nucleus, it can be expected that the restoring force can be modelled to be linear. Thus it can be safely assumed that our linear spring model is a good enough approximation for the physical reality of real experiments.

In the previous section, section 4.1. Where the horizontal spring model was discussed, the linear spring approximation was already mentioned, but not yet justified. A similar calculation could be done for that case, resulting in a comparable confirmation of what is now justifiably assumed to be valid.

4.2.3. Restoring force

The spring force of a single spring is calculated as follows.

$$F_s = k(L - L_R) = k(L_0 + \frac{u^2}{2L_0} - L_R) \tag{4.9}$$

Where L_R is the relaxed length of the spring and k the spring constant. From equation 4.9 the following pretension force T is defined.

$$T \equiv k(L_0 - L_R) \tag{4.10}$$

Using the spring force from equation 4.9 and the angle θ the vertical component of the spring force for either spring, the restoring force F_r, can be calculated.

$$F_r = F_s \sin(\theta) = F_s \frac{u}{L} \approx k(L_0 + \frac{u^2}{2L_0} - L_R)\frac{u}{L} \tag{4.11}$$

Let's now rewrite $\frac{1}{L}$ in this equation to something more convenient

$$\frac{1}{L} \approx \frac{1}{L_0 + \frac{u^2}{2L_0}} = \frac{1}{L_0}\frac{1}{1 + \frac{u^2}{2L_0^2}} \tag{4.12}$$

Now another Taylor expansion can be applied using the same assumption $L_0 \gg u$ to get the following equation

$$\frac{1}{L} \approx \frac{1}{L_0}\left(1 - \frac{u^2}{L_0^2}\right) \tag{4.13}$$

Plugging this into equation 4.11 the following approximation can be obtained.

$$F_r \approx k\left(L_0 - L_R + \frac{u^2}{2L_0}\right)\frac{u}{L_0}\left(1 - \frac{u^2}{L_0^2}\right) = k\frac{L_0 - L_R}{L_0}u + k\left(1 - 2\frac{L_0 - L_R}{L_0}\right)\frac{u^3}{2L_0^2} - k\frac{u^5}{2L_0^4} \tag{4.14}$$

Because the amplitudes u will be small the higher order term which scales with u^5 can be neglected. You might be tempted to also neglect the other non-linear term which scales with u^3. But this term can actually be larger than the linear term, depending on the value for the pretension force. Without pretension force the linear term drops out completely The derived restoring force is that which only one spring contributes. Now assuming that both springs balance each other horizontally, or to put it in other words, assuming that both springs have the same spring constant, a net force F_R can be found.

$$F_R \approx -2k\frac{L_0 - L_R}{L_0}u - k\left(1 - 2\frac{L_0 - L_R}{L_0}\right)\frac{u^3}{L_0^2} \tag{4.15}$$

The net force is taken to be negative because it is pointed opposite to the displacement (vector).

4.2.4. Structural damping

In this section the structural damping will be studied, specifically the alteration in the structural damping when the mass is oscillating transversally instead of horizontally. This alteration is basically the same as that in the previous section, section 4.2.3, but now the k includes the same loss angle term $\phi(\omega)$ as was introduced in section 3.2. Introducing the loss angle here has to be done with care, because only the forces which depend on the velocity should include a structural damping term. To illustrate this point first a *wrong approach* will be taken

Wrong approach

$$F_R^{in} = F_R\left[1 + i\phi(\omega)\right] \approx -2k\left[1 + i\phi(\omega)\right]\frac{L_0 - L_R}{L_0}u - k\left[1 + i\phi(\omega)\right]\left(1 - 2\frac{L_0 - L_R}{L_0}\right)\frac{u^3}{L_0^2} \tag{4.16}$$

Now that the force includes the internal damping the equations of motion for the vertical motion can be formed.

$$m\ddot{u} = \sum_i F_i \approx -2k\left[1 + i\phi(\omega)\right]\frac{L_0 - L_R}{L_0}u - k\left[1 + i\phi(\omega)\right]\left(1 - 2\frac{L_0 - L_R}{L_0}\right)\frac{u^3}{L_0^2} \tag{4.17}$$

Obtaining the following second order linear homogeneous differential equation with variable coefficients.

$$m\frac{d^2u}{dt^2} + 2k\left[1 + i\phi(\omega)\right]\frac{L_0 - L_R}{L_0}u + k\left[1 + i\phi(\omega)\right]\left(1 - 2\frac{L_0 - L_R}{L_0}\right)\frac{u^3}{L_0^2} \approx 0 \tag{4.18}$$

The wrong Loss tangent

To determine the loss tangent, of the springs described in this model, the spring constant has to be split in its purely real and imaginary parts.

$$k = k' - ik'' \tag{4.19}$$

Let's rewrite equation 4.18 to see what can be obtained for k' and k''

$$\begin{aligned}
0 &\approx m\frac{d^2u}{dt^2} + 2k\left[1 + i\phi(\omega)\right]\frac{L_0 - L_R}{L_0}u + k\left[1 + i\phi(\omega)\right]\left(1 - 2\frac{L_0 - L_R}{L_0}\right)\frac{u^3}{L_0^2} \\
k\left[1 + i\phi(\omega)\right] &\approx -m\frac{d^2u}{dt^2}\cdot\left[2\frac{L_0 - L_R}{L_0}u + \left(1 - 2\frac{L_0 - L_R}{L_0}\right)\frac{u^3}{L_0^2}\right]^{-1} \\
k &\approx \beta - i\beta\phi(\omega); \text{ with } \beta \equiv -m\frac{d^2u}{dt^2}\cdot\left[1 + \phi^2(\omega)\right]^{-1}\left[2\frac{L_0 - L_R}{L_0}u + \left(1 - 2\frac{L_0 - L_R}{L_0}\right)\frac{u^3}{L_0^2}\right]^{-1} \\
k' &\approx \beta \quad \wedge \quad k'' \approx \beta\phi(\omega)
\end{aligned} \tag{4.20}$$

The lag function can now again be found by dividing the k' into k''. And again a constant $\phi(\omega)$ is found.

$$\phi(\omega) = \frac{k''}{k'} = \tan(\delta) \tag{4.21}$$

But this is wrong! This result is just the same as what was found for the horizontal spring model, and it seems as if you would always find a constant $\phi(\omega)$ for any linear system. But what went wrong? It happened in equation 4.16, al the way at the start of this attempt to find the behaviour of structural damping. There the spring constant was rewritten, as was done before in equation 4.2. It complies with the following transformation: $k \to k\left[1 + i\phi(\omega)\right]$. But this transformation can only be done if the spring constant is a proper one. So a constant which relates a positional coordinate to a certain restoring force. It makes sense to do the transformation for such cases because the damping relates to the decrease of the amplitude and the maximum restoring force. Now that this has been found a new approach can be made.

Correct approach

To do the transformation of the spring constant it is best to start with the simplest equation of the restoring force, equation 4.9.

$$\begin{aligned}
F_s &= k(L - L_R) \\
F_s &= k(L_0 - L_R + x) \\
F_s &= k(L_0 - L_R) + kx
\end{aligned} \tag{4.22}$$

Now by splitting the equation into two parts it can be observed that only the second part depends on a positional coordinate. The pretension force should not change under transformation of the spring constant, thus the transformation is only applied on the second term.

$$F_s^{in} = k(L_0 - L_R) + k\left[1 + i\phi(\omega)\right]x \tag{4.23}$$

And now all that is left is to work this formula out, this is very similar to what was done in section 4.2.3. In the end the following equation is obtained.

$$F_R^{in} \approx -2k\frac{L_0 - L_R}{L_0}u + k\frac{L_0 - L_R}{L_0^2}u^3 - k\frac{1}{L_0^2}\left[1 + i\phi(\omega)\right]u^3 \tag{4.24}$$

So, now it can be noticed that there is no damping in the linear restoring force. The damping occurs in the higher order terms, which is great because these can be disregarded for small amplitudes.

Loss tangent & Quality factor for the correct approach

To calculate the loss tangent the real and imaginary parts of the spring constant have to be determined. For the linearised restoring force there is no imaginary part. Thus the loss tangent will approximately be zero, $\tan(\delta) \approx 0$. This also means that the Q-factor will be infinite, $Q \approx \infty$.

How can this result of infinite Q be interpreted? Well when compared to the constant Q that was found for the horizontal spring model, in section 4.1.3, it can be said that horizontal oscillation modes in the beam will die out quicker than the vertical ones. Where only the effect of the elongation of the beam is taken into account. But this is not the full story yet. When the beam oscillates in the vertical direction it bends. Due to the bending stiffness of the beam it will try and resist this bending. This results not only in a transverse force due to the elongation. It also delivers a torsional force due to angular deformation.

4.3. Torsion in transverse motion

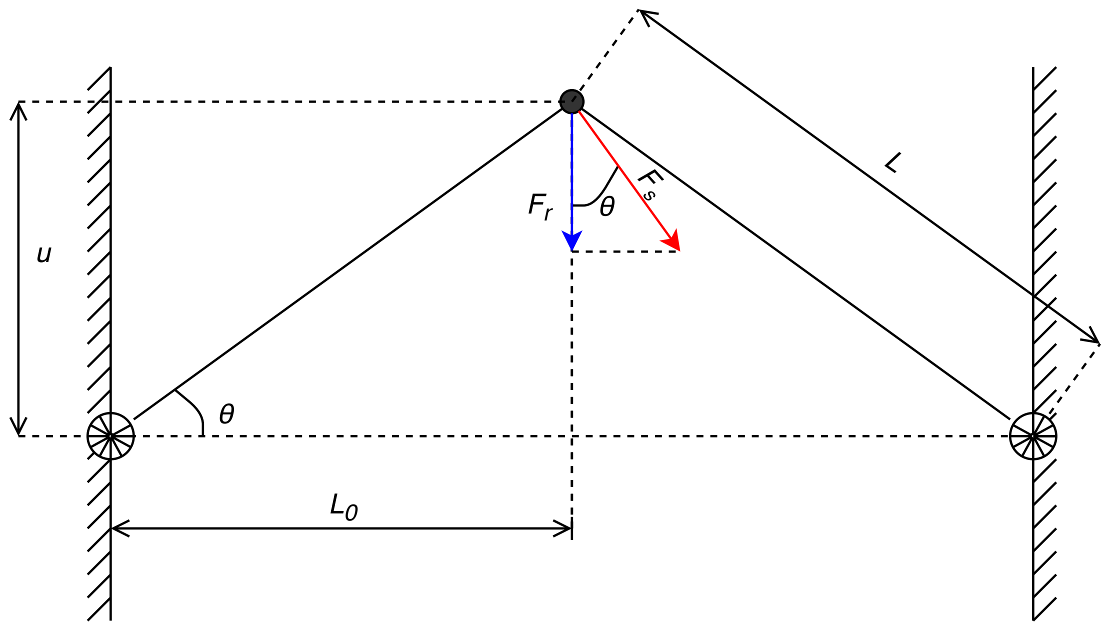

Figure 4.3: Schematic overview of the simple torsion spring model. Here it is assumed that the beams connecting the torsion springs to the mass can freely stretch and contract.

4.3.1. Angular deformation

In figure 4.3 a schematic drawing can be seen of the oscillating mass attached with two torsion springs. It is assumed that the mass is in the middle, located a distance L_0 from the sides. Note that for torsion springs the force depends on the angle θ. The elongation of the spring doesn't directly influence the torsion spring force F_s. However, because the mass in this model is bound to one horizontal coordinate L_0, θ does depend on the elongation of the springs.

At a certain time t the mass is at height u, the springs connected to the mass now make an angle θ with the horizontal axis. Notice how similar figure 4.2 and 4.3 look, this is done on purpose so later the results of these models can be combined. Because they are so similar the equations 4.5, 4.6, 4.7 and 4.8 also apply in this model. By applying some trigonometry to the triangle created by the sides with length u and L along with the angle θ, a relation can be found between these three variables.

$$\sin(\theta) = \frac{u}{L} \tag{4.25}$$

To further simplify equation 4.25 a Taylor expansion is done for the following situation: $L_0 \gg u$, this simplifies the left-hand side of equation 4.25. Equation 4.13 also holds here, but it can be even further simplified because the term $\frac{u^2}{L_0^2}$ will also vanish in this model. This is because ΔL does not play a role here and thus later on the linear term cannot be set to zero, making it always dominate the higher order terms. Thus the following is obtained

$$\theta \approx \frac{u}{L} \approx \frac{u}{L_0} \tag{4.26}$$

4.3.2. Restoring force

The torsion spring applies a torque τ on the mass m. The general definition of a torque $\vec{\tau}$ is given by

$$\vec{\tau} \equiv \vec{r} \times \vec{F} \tag{4.27}$$

where $\vec{r}$ is the position vector of the point mass relative to the pivot point, and $\vec{F}$ is the force acting on the mass. Because $\vec{r}$ and $\vec{F}$ are perpendicular, and applying equation 4.13 again the magnitude of $\vec{F}$ is given by

$$F_s = \frac{\|\vec{\tau}\|}{L} \approx \frac{\|\vec{\tau}\|}{L_0} \tag{4.28}$$

For the magnitude of $\vec{\tau}$ it is known that the torsion springs obey an angular form of Hooke's law

$$\tau_s = \kappa\theta \tag{4.29}$$

Wherein κ is the torsion coefficient of the spring. It is assumed that both springs have the same torsion coefficient. Thus both springs deliver a force $F_{s,i}$ that can be projected onto the vertical axis to obtain a total restoring force F_R. The force $F_{s,1}$ that the left torsion spring applies here is perpendicular to the beam that connects the mass to the pivot point. By projecting this force on the vertical axis a vertical restoring force $F_{r,1}$ is obtained. The same can be done for the right spring to obtain the total restoring force F_R. All that is needed for this is some trigonometry on the little triangle, created by connecting the two ends of F_s and F_r. Again the convention of having the net force pointed opposite to the displacement is applied.

$$F_R = -F_{r,1} - F_{r,2} = -\left(F_{s,1} + F_{s,2}\right)\cos(\theta) \tag{4.30}$$

This equation can further be simplified by doing another Taylor expansion, this time for $\cos(\theta)$, and because only the linear term is of interest $\cos(\theta) \approx 1$ will suffice. Furthermore, equation 4.26 and 4.29 can be filled in to obtain

$$\begin{aligned}
F_R &= -\left(F_{s,1} + F_{s,2}\right)\cos(\theta) \\
F_R &\approx -F_{s,1} - F_{s,2} \\
F_R &\approx -\frac{\tau_{s,1}}{L_0} - \frac{\tau_{s,2}}{L_0} \\
F_R &\approx -2\frac{\kappa}{L_0}\theta \approx -2\frac{\kappa}{L_0^2}u
\end{aligned} \tag{4.31}$$

It is now seen that the resulting restoring force due to torsion springs is linear, similar to the restoring force in the horizontal spring model.

4.3.3. Structural damping

Now the alteration of structural damping for the torsion springs can be studied, in a similar fashion as in section 4.1.3, making a slight adjustment to what was done before in section 3.2.

$$F_R^{in} = F_R \left[1 + i\phi(\omega)\right] \approx -2\frac{\kappa}{L_0^2}\left[1 + i\phi(\omega)\right] u \tag{4.32}$$

Now that the force includes the internal damping the equations of motion for the vertical motion can be formed.

$$m\ddot{u} = \sum_i F_i \approx -2\frac{\kappa}{L_0^2}\left[1 + i\phi(\omega)\right] u \tag{4.33}$$

Obtaining the following second order linear homogeneous differential equation with variable coefficients.

$$m\frac{d^2u}{dt^2} + 2\frac{\kappa}{L_0^2}\left[1 + i\phi(\omega)\right] u \approx 0 \tag{4.34}$$

The damping in the vertical direction is found, and it is linearly damped. From this the Fourier transformed differential equation can be obtained.

$$m(i\omega)^2 U(\omega) + 2\frac{\kappa}{L_0^2}\left[1 + i\phi(\omega)\right] U(\omega) \approx 0 \tag{4.35}$$

Again the only thing that changes from the previously obtained solution is the undamped angular frequency ω_0.

$$\omega_0 = \sqrt{\frac{2\kappa}{mL_0^2}} \tag{4.36}$$

And for u the following is found.

$$u(t) \approx \alpha\, e^{-\frac{1}{2}\omega_0\phi(\omega)\cdot t}\, e^{i\omega_0\left(1+\frac{\phi^2(\omega)}{8}\right)\cdot t+\varphi} \tag{4.37}$$

Loss tangent & Quality factor

To obtain the loss tangent and the quality factor the same calculation as in section 3.2.2 can be repeated for this model. The result will be the same, a constant loss tangent and quality factor.

4.4. Stretching & torsion in transverse motion

The model described in this section can be seen as the sum of the stretching and torsion spring models, which were described in section 4.2 and 4.3 respectively. By applying the superposition principle, it can be said that the response caused by the two spring models is simply the sum of the responses that would have been caused by each spring model individually [8]. This principle will be used throughout this section to combine the previous models to construct a more complete beam model.

4.4.1. Combined deformation

In figure 4.4 a schematic drawing can be seen of the oscillating mass attached with four springs, two transverse and two torsion springs. It is assumed that the mass is in the middle, located a distance L_0 from the sides. At a certain time t the mass is at height u, the springs connected to the mass now make an angle θ with the horizontal axis. The equations 4.8 and 4.26 can now be used to relate the variables x, u, L_0 and θ to each other, wherein L_0 is a constant parameter depending on the set-up of the experiment

4.4.2. Restoring force

The total restoring force can simply be obtained by summing the restoring forces from the previous models together. So by summing equations 4.15 and 4.31 the following equation is found.

$$F_R \approx -2\frac{\kappa}{L_0^2}u - 2k\frac{L_0 - L_R}{L_0}u - k\left(1 - 2\frac{L_0 - L_R}{L_0}\right)\frac{u^3}{L_0^2} \tag{4.38}$$

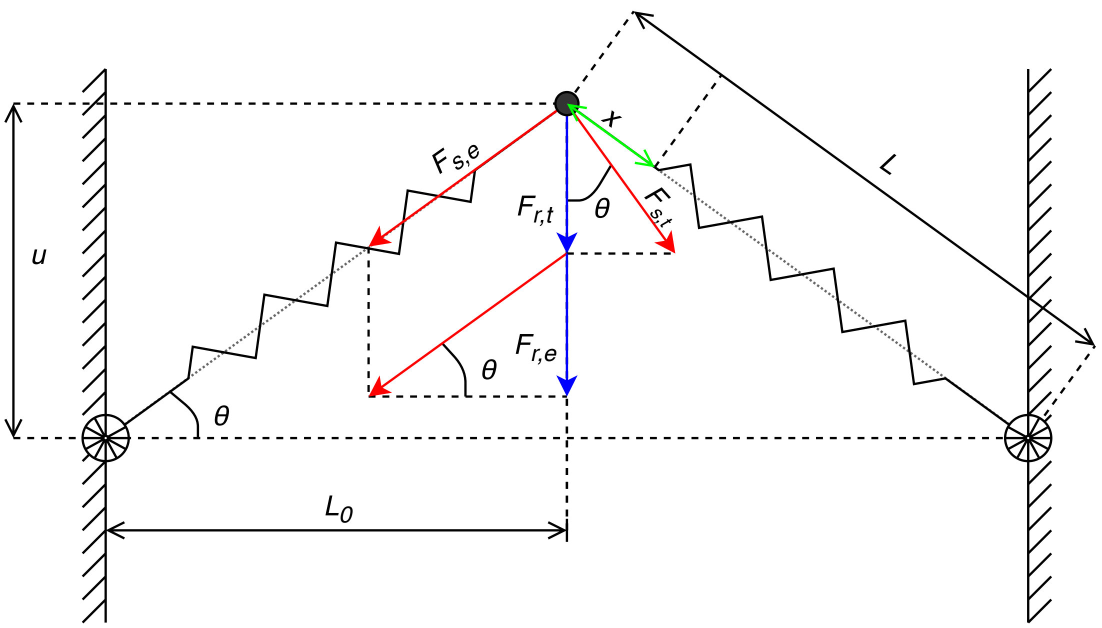

Figure 4.4: Schematic overview of the combined transverse stretching and torsion spring model.

4.4.3. Structural damping

Because the total restoring force is simply the sum of the restoring forces from the previous models, the structural damping is obtained in a similar way. The following formula can be obtained.

$$F_R^{in} \approx -2\frac{\kappa}{L_0^2}\left[1+i\phi_\kappa(\omega)\right]u - 2k\frac{L_0-L_R}{L_0}u + 2k\frac{L_0-L_R}{L_0}\frac{u^3}{L_0^2} - k\left[1+i\phi_k(\omega)\right]\frac{u^3}{L_0^2}$$
$$F_R^{in} \approx -2\frac{\kappa}{L_0^2}\left[1+i\phi_\kappa(\omega)\right]u - 2k\frac{L_0-L_R}{L_0}u \tag{4.39}$$

The non-linear terms have been thrown out of the equation because these will be small compared to the rest of the terms. Now that the force includes the internal damping the equations of motion for the vertical motion can be formed.

$$m\ddot{u} = \sum_i F_i \approx -2\frac{\kappa}{L_0^2}\left[1+i\phi_\kappa(\omega)\right]u - 2k\frac{L_0-L_R}{L_0}u \tag{4.40}$$

Obtaining the following second order linear homogeneous differential equation with variable coefficients.

$$m\frac{d^2u}{dt^2} + 2\frac{\kappa}{L_0^2}\left[1+i\phi_\kappa(\omega)\right]u + 2k\frac{L_0-L_R}{L_0}u \approx 0 \tag{4.41}$$

So two linear terms are found of which only the one coming from the torsion model includes a damping factor. To further simplify the model it is assumed that both springs contribute equally to the vertical restoring force when there is no initial strain: $L_0 - L_R = 0 \rightarrow k = \frac{\kappa}{L_0^2} \equiv K$

$$m\frac{d^2u}{dt^2} + 2K\left\{\left[1+i\phi_\kappa(\omega)\right] + \frac{L_0-L_R}{L_0}\right\}u \approx 0 \tag{4.42}$$

The next step will be to solve equation 4.42 and obtain a formula for $u(t)$. To do this, the previous ansatz from equation 3.16 can be used again. Again following the same procedure as in section 3.2.

$$m(i\omega)^2 U(\omega) + 2K\left\{\left[1+i\phi_\kappa(\omega)\right] + \frac{L_0-L_R}{L_0}\right\}U(\omega) \approx 0 \tag{4.43}$$

Equation 4.43 can be simplified by factoring out the $U(\omega)$ term.

$$m(i\omega)^2 U(\omega) + 2K\left\{\left[1+i\phi_\kappa(\omega)\right] + L_0\left(L_0 - L_R\right)\right\} U(\omega) \approx 0$$
$$\left(m(i\omega)^2 + 2K\left\{\left[1+i\phi_\kappa(\omega)\right] + \frac{L_0 - L_R}{L_0}\right\}\right) U(\omega) \approx 0$$
$$m(i\omega)^2 + 2K\left\{\left[1+i\phi_\kappa(\omega)\right] + \frac{L_0 - L_R}{L_0}\right\} \approx 0 \quad \vee \quad U(\omega) \approx 0 \ \text{(The trivial solution)} \tag{4.44}$$

From the trivial solution it can be seen that it holds only if $\omega \neq i\lambda$. In the case that $\omega = i\lambda$, a solution for λ can be obtained.

$$\lambda_\pm \approx \pm i\sqrt{\frac{2K}{m}}\sqrt{\left[1+i\phi_\kappa(\omega)\right] + \frac{L_0 - L_R}{L_0}} \tag{4.45}$$

Now for the same reason as before only λ_+ is considered. Let's calculate the real and imaginary part of this eigenvalue so that these terms can be split.

$$\lambda_+ \approx i\sqrt{\frac{2K}{m}}\sqrt{\left[1+i\phi_\kappa(\omega)\right] + \frac{L_0 - L_R}{L_0}} = i\omega_0\sqrt{z} \rightarrow \sqrt{z} = \sqrt{r\left(\cos(\theta) + i\sin(\theta)\right)}$$
$$\text{with } r = \sqrt{\left(1+\frac{L_0 - L_R}{L_0}\right)^2 + \phi_\kappa^2(\omega)};\quad \cos(\theta) = \frac{1}{r}\left(1+\frac{L_0 - L_R}{L_0}\right);\quad \sin(\theta) = \frac{\phi_\kappa(\omega)}{r}$$
$$\lambda_+ \approx \frac{1}{2}\sqrt{2}i\omega_0\left\{\sqrt{\sqrt{\left(1+\frac{L_0 - L_R}{L_0}\right)^2 + \phi_\kappa^2(\omega)} + 1 + \frac{L_0 - L_R}{L_0}} + \right.$$
$$\left. i\sqrt{\sqrt{\left(1+\frac{L_0 - L_R}{L_0}\right)^2 + \phi_\kappa^2(\omega)} - 1 - \frac{L_0 - L_R}{L_0}}\right\}$$
$$\lambda_+ \approx \frac{1}{2}\sqrt{2}i\omega_0\left\{\sqrt{\sqrt{\gamma^2 + \phi_\kappa^2(\omega)} + \gamma} + i\sqrt{\sqrt{a^2 + \phi_\kappa^2(\omega)} - \gamma}\right\};\quad \text{with } \gamma = 1 + \frac{L_0 - L_R}{L_0}$$
$$\lambda_+ \approx \frac{1}{2}\sqrt{2}i\omega_0\left\{\sqrt{2\gamma + \frac{\phi_\kappa^2(\omega)}{2\gamma}} + i\sqrt{\frac{\phi_\kappa^2(\omega)}{2\gamma}}\right\}$$
$$\lambda_+ \approx i\omega_0\left\{\sqrt{\gamma} + \frac{\phi_\kappa^2(\omega)}{8\gamma^{3/2}} + \frac{i\phi_\kappa(\omega)}{2\sqrt{\gamma}}\right\}$$
$$\lambda_+ \approx -\frac{1}{2\sqrt{\gamma}}\omega_0\phi_\kappa(\omega) + i\omega_0\sqrt{\gamma}\left(1+\frac{\phi_\kappa^2(\omega)}{8\gamma^2}\right)$$
$$\mathfrak{Re}\{\lambda_+\} \approx -\frac{1}{2\sqrt{\gamma}}\omega_0\phi_\kappa(\omega) \quad \wedge \quad \mathfrak{Im}\{\lambda_+\} \approx \omega_0\sqrt{\gamma}\left(1+\frac{\phi_\kappa^2(\omega)}{8\gamma^2}\right) \tag{4.46}$$

Thus for u the following is found:

$$u(t) \approx \alpha\, \mathrm{e}^{-\frac{1}{2\sqrt{\gamma}}\omega_0\phi_\kappa(\omega)\cdot t}\, \mathrm{e}^{i\omega_0\sqrt{\gamma}\left(1+\frac{\phi_\kappa^2(\omega)}{8\gamma^2}\right)\cdot t+\varphi} \tag{4.47}$$

Note that the frequency ω of the oscillation is given by: $\omega = \omega_0\sqrt{\gamma}\left(1+\frac{\phi_\kappa^2(\omega)}{8\gamma^2}\right)$. It depends on both ω_0, $\phi_\kappa(\omega)$ and the relative initial strain γ.

Loss tangent & Quality factor

To determine the loss tangent and quality factor, of the springs described in this model, the spring constant has to be split in its purely real and imaginary parts.

$$K = K' - iK'' \tag{4.48}$$

Let's rewrite equation 4.41 to see what can be obtained for K' and K''.

$$\begin{aligned}
m\frac{d^2u}{dt^2} + 2K\left\{\left[1+i\phi_\kappa(\omega)\right] + \frac{L_0-L_R}{L_0}\right\}u \approx 0 \\
K\left\{\left[1+i\phi_\kappa(\omega)\right] + \frac{L_0-L_R}{L_0}\right\} \approx -\frac{1}{2u}m\frac{d^2u}{dt^2} \\
K \approx -\frac{1}{2u}m\frac{d^2u}{dt^2}\left\{\left[1+i\phi_\kappa(\omega)\right] + \frac{L_0-L_R}{L_0}\right\}^{-1}
\end{aligned}$$

Let's rewrite the term in the curly brackets to split it in a purely real and imaginary part. The substitution for the relative initial strain is used again: $\gamma = 1 + \frac{L_0-L_R}{L_0}$.

$$\frac{1}{\gamma+i\phi_\kappa(\omega)} = \frac{1}{\gamma+i\phi_\kappa(\omega)}\cdot\frac{\gamma-i\phi_\kappa(\omega)}{\gamma-i\phi_\kappa(\omega)} = \frac{\gamma}{\gamma^2+\phi_\kappa^2(\omega)} - i\frac{\phi_\kappa(\omega)}{\gamma^2+\phi_\kappa^2(\omega)}$$

Now this can be used in the equation for K:

$$\begin{aligned}
&K \approx \beta\gamma - i\beta\phi_\kappa(\omega);\quad \text{with } \beta \equiv -\frac{1}{2u}m\frac{d^2u}{dt^2}\frac{1}{\gamma^2+\phi_\kappa^2(\omega)} \\
&K' \approx \beta\gamma \quad\wedge\quad K'' \approx \beta\phi_\kappa(\omega)
\end{aligned} \tag{4.49}$$

The loss tangent can now simply be found by dividing the K' into K''.

$$\tan(\delta) = \frac{K''}{K'} = \frac{\phi_\kappa(\omega)}{\gamma} \tag{4.50}$$

What is found is almost the same equation as before, but now the loss tangent depends on an additional factor. The relative initial strain, which is determined by the length of the springs and their rest length.

The Q-factor can now easily be calculated by inverting these variables as seen in equation 3.12.

$$Q = \frac{K'}{K''} = Q_\kappa\cdot\left[1+\frac{L_0-L_R}{L_0}\right] \tag{4.51}$$

So now we see that the Q-factor increases if the strain in the beam would increase. Which is one of the expected characteristics of oscillating beams.

4.5. Plots & Discussion

Effective spring constant

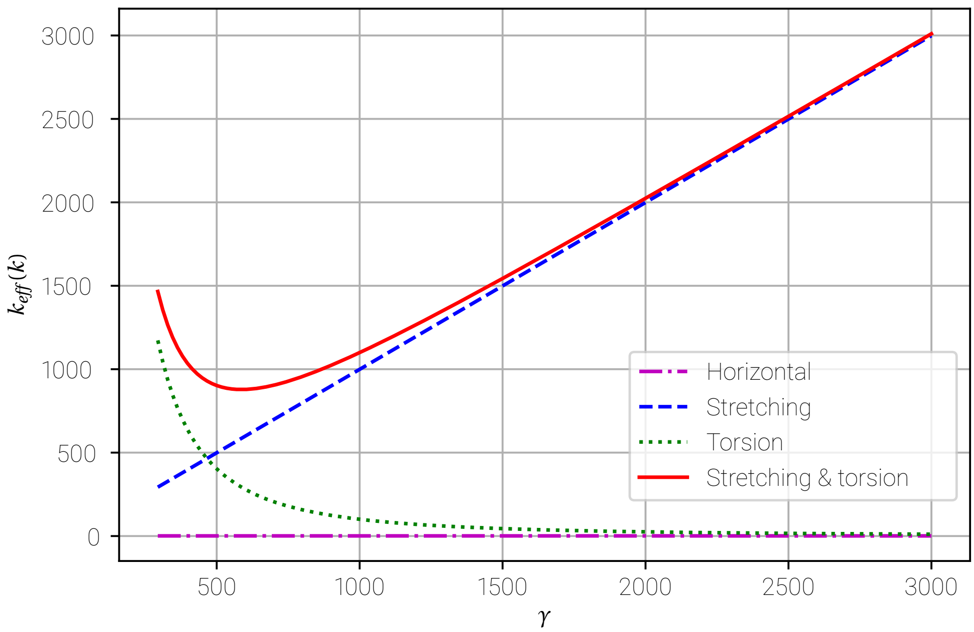

Figure 4.5: In this graph the effective k, k_{eff}, of the discussed spring models are plotted versus the relative initial strain γ. k_{eff} is given in units of the horizontal spring constant k. The following values have been used to create this graph, $L_0 = 100\mu m$ and L_R is in a range from -2998 to -292 L_0. For the torsion plot to obtain the same γ, L_R is taken as a constant and L_0 is varied, $L_R = -100\mu m$ and L_0 is in a range from -2998 to -292 L_R.

To visualize the calculations described in this chapter two figures have been made. Figure 4.5 shows the plots of k_{eff} vs γ for these models. The effective spring constant encapsulates the variables that aren't part of the standard spring constant, so that the resulting responsive forces to a certain amplitude of the models can be compared.

The effective spring constant of the horizontal model, displayed as a purple dash-dotted line, is taken as the baseline, as it is constant and its spring constant is generally the weakest (except for long torsion springs).

The effective spring constant of the transverse stretching spring model is displayed as a blue dashed line. It increases linearly as the strain is increased, mathematically towards infinity, physically to a certain k_{max} constrained by the maximum strain for which the system still behaves elastically.

The torsion model's k_{eff} is portrayed by the green dotted line. It decreases as a quadratic rational function towards zero.

The effective spring constant of the combined stretching and torsion model is now simply obtained as the sum of those for the separate models. It is displayed as the red line. For low γ the springs will behave similar to torsion springs, while at high γ they will behave more like tension springs.

The quality factor

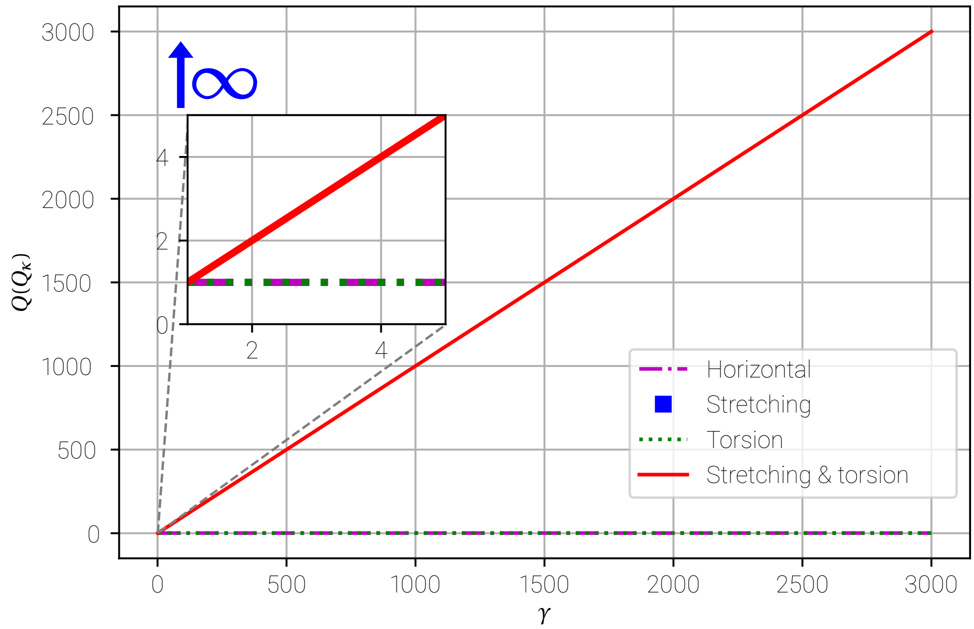

Figure 4.6: In this graph the Q-factor is plotted versus the relative initial strain γ. The following values have been used to create this graph, $L_0 = 100\mu m$ and L_R is in a range from -2998 to 1 L_0. For the torsion plot to obtain the same γ, L_R is taken as a constant and L_0 is varied, $L_R = -100\mu m$ and L_0 is in a range from -2998 to 1 L_R.

Figure 4.6 shows the plots of Q vs γ for the described spring systems. The loss tangents of the respective models can be inferred from these Q-factors. In this way the resonance behaviour and the qualitative damping process of the spring systems can be compared.

The Q-factor of the horizontal model, displayed as a purple dash-dotted line, is exactly the same as the torsion model's Q-factor portrayed by the green dotted line. Because, in both systems the imaginary and real part of the spring constants only vary by the loss angle $\phi(\omega)$. These lines are part of the common baseline, which is equal to the constant value of Q_κ

The Q-factor of the transverse stretching spring model is displayed as a blue arrow pointing towards infinity. For the linearised restoring force there was no imaginary component. Thus for small amplitudes, the loss tangent for this system is zero. And because the force depends linearly on the strain for zero strain there is no restoring force, so the resonator will come to a standstill. So at $\gamma = 1$ there is no Q-factor for this system to define. So, mathematically the system has infinite Q, but physically there will be a certain Q depending on the imaginary and real components of the higher order terms.

The Q-factor of the combined stretching and torsion model is obtained by equation 4.51. It is displayed as the red line. It can be observed that the Q-factor of the combined system increases linearly with the strain. And again, similar to the k_{eff}, it increases towards infinity, but physically it should increase to a certain Q-factor constrained by the maximum strain for which the system still behaves elastically.

5
Conclusion

To conclude, the goal of the research described in this thesis was to investigate the basis of dissipation dilution as well as make it comprehensible. In the written literature we could find that the kinetic energy of an oscillating beam is stored into two types of potential energy [4, 5]. A dissipative bending component and a conservative component due to elongation.

After this the different types of damping were introduced. Of which structural damping was most important, it is experimentally found to be approximately constant for many materials over a large band of frequencies. The loss tangent and quality factor for this type of damping are both constant. The physical origin of this behaviour isn't really understood. But there have been ideas hinted that it is due to surface imperfections [5].

To simulate dissipation dilution a spring system has been developed. In this system part of the energy is stored in torsion springs and another part in elongation springs. From this model it is observed that the effective spring constant of the total system depends on the initial strain. At low amounts of strain the spring constant is similar to that of torsion springs while at higher strains it becomes more like the elongation spring model. The quality factor of the beam is found to increase linearly with the strain.

So, just like a guitar, the nanomechanical resonator has to be tuned so that it produces the desired resonance behaviour. But unlike the guitar the frequency that is sought after is fundamentally different.

Bibliography

[1] R. C. Hibbeler. *Mechanics of Materials.* Pearson Education, 2003.

[2] Leonardo da Vinci. *Codex Madrid I.* McGraw-Hill Book Company, 1493. [Accessed 15-July-2019].

[3] Jooinn. Guitar strings 2. Available at: `https://jooinn.com/guitar-strings.html`. [Accessed 15-July-2019].

[4] Quirin P. Unterreithmeier, Thomas Faust, and Jörg P. Kotthaus. Damping of nanomechanical resonators. *Phys. Rev. Lett.*, 105(2):027205, July 2010.

[5] A. H. Ghadimi, S. A. Fedorov, N. J. Engelsen, M. J. Bereyhi, R. Schilling, D. J. Wilson, and T. J. Kippenberg. Elastic strain engineering for ultralow mechanical dissipation. *Science*, 360(6390):764–768, May 2018.

[6] Peter R. Saulson. Thermal noise in mechanical experiments. *Phys. Rev. D*, 42:2437–2445, October 1990.

[7] A. Mostowski; M. Stark. *Introduction to Higher Algebra.* Pergamon Press, 1964.

[8] Valerie Illingworth. *The Penguin Dictionary of Physics.* Penguin Books, L, 1991.